

# QUANTUM AND TRANSPORT SCATTERING TIMES IN AlGaAs/InGaAs NANOHETEROSTRUCTURES WITH AIAs INSERTS IN THE SPACER LAYER

G.B. Galiev <sup>a</sup>, I.S. Vasil'evskii <sup>b</sup>, E.A. Klimov <sup>a</sup>, D.S. Ponomarev <sup>a</sup>, R.A. Khabibullin <sup>a</sup>,

V.A. Kulbachinskii <sup>c</sup>, D.V. Gromov <sup>b</sup>, and P.P. Maltsev <sup>a</sup>

<sup>a</sup> *Institute of Ultra High Frequency Semiconductor Electronics of Russian Academy of Sciences, Nagornyi pr. 7,  
117105 Moscow, Russia*

<sup>b</sup> *Moscow Engineering Physics Institute (MEPhI) – National Research Nuclear University, Kashirskoe sh. 31,  
115409 Moscow, Russia*

<sup>c</sup> *M.V. Lomonosov Moscow State University, Moscow, GSP-1, 119991 Russia*

E-mail: ponomarev@isvch.ru

Received 22 May 2015; accepted 29 September 2015

The influence of nano-sized AIAs inserts in the spacer layer AlGaAs on scattering mechanisms of AlGaAs/InGaAs nanoheterostructures has been considered. It was shown that the introduction of AIAs lead to mobility enhancement up to 20%. The ratio of transport-to-quantum scattering times revealed that in the case of the spacer with AIAs inserts the scattering on ionized Si-donors is strongly decreased in comparison to the spacer without AIAs.

**Keywords:** AIAs inserts, quantum and transport scattering times, scattering mechanisms, nanoheterostructure

**PACS:** 68.55.ag, 68.65.Fg, 72.80.Ey

## 1. Introduction

InGaAs-based heterostructures are well-suited for high electron mobility transistors (HEMTs). Two-dimensional electron gas (2DEG) confined to a quantum well (QW) InGaAs demonstrates both high electron mobility and drift velocity. The most important factors that limit electron mobility  $\mu_e$  in HEMT are the polar optical phonon scattering [1, 22] and remote ionized impurity scattering [3]. In order to improve  $\mu_e$  one should vary the design of the heterostructure, in particular the QW and the barrier layer. One of the approaches is the introduction of additional InAs and/or GaAs layers that lead to decreasing of electron effective mass in the QW but enhance scattering on the interface roughness [4]. Previously it was shown that Al-

GaAs/InGaAs heterostructures with the QW containing AIAs inserts that serve as the barriers for optical phonons may reduce the scattering rate up to 5–6 times in comparison with the QW without these inserts and increase electron mobility as a consequence [5, 6]. Nevertheless, the influence of these nanoinserts on the scattering mechanisms should be studied more elaborately. One of the approaches is to measure transport-to-quantum scattering times ratio of the heterostructures [7, 8].

The difference between two scattering times is in the averaging of the dominant scattering events over all scattering angles. The transport scattering time  $\tau_t$  is a measure of the amount of time a carrier remains moving in a particular direction. In contrast, the quantum scattering time  $\tau_q$  is a measure of the mean time a carrier remains in a particular state

before being scattered to a different state and therefore all scattering events are weighted equally in calculation of  $\tau_q$ . The both times are given by [9, 10]

$$\frac{1}{\tau_q} = \frac{m^*}{\pi \hbar^3} \int_0^\pi d\Theta |V(q)|^2, \quad (1)$$

$$\frac{1}{\tau_t} = \frac{m^*}{\pi \hbar^3} \int_0^\pi d\Theta |V(q)|^2 (1 - \cos(\Theta)), \quad (2)$$

where  $\Theta$  is the scattering angle,  $q = 2k_F \sin(\Theta/2)$ , the Fermi wave vector  $k_F = \sqrt{2\pi n_s}$ ,  $n_s$  is electron concentration in QW, and  $V(q)$  is the probability of scattering through an angle  $\Theta$  from one state to another on the Fermi circle. As seen from Eqs. (1) and (2), the inclusion of a factor  $(1 - \cos(\Theta))$  emphasizes the importance of the large angle over small angle scattering events. Therefore the ratio  $\tau_t/\tau_q$  gives information about the dominant scattering mechanisms that restrict electron mobility in QW.

For the short-term scattering potential attributed to alloy disorder and surface roughness,  $V(q)$  is an isotropic function of the scattering angle and  $\tau_t/\tau_q \sim 1$ , while for the long-term scattering potential, for instance, scattering on remote ionized impurity,  $\tau_t/\tau_q \gg 1$  [11]. It should be noticed that  $\tau_q$  does not depend on temperature at  $T < 40$  K [12] that relates to scattering of the degenerated 2DEG on remote ionized impurity. Also,  $\tau_q$  slowly decreases with the reduction of the carrier wave function width due to a strong spatial confinement of carriers in the QW [13]. It was also reported [14] that scattering centers are close to 2DEG when  $\tau_t/\tau_q \sim 3$  and the Coulomb scattering between partially ionized donors and 2D electrons in the QW predominates alloy disorder scattering.

One of the approaches leading to enhancement of the carriers transport in modulation-doped heterostructures is the increasing of the spacer layer thickness, i. e. separating the ionized donor atoms further away from 2DEG in the QW. This means that a large or moderate-angle scattering has been replaced by a small-angle scattering so that the mobility, which is weighted towards large-angle-scattering events, is increased [15]. However, the spacer thickness  $d_{sp}$  is limited due to appearance of the parallel conductivity when the V-shaped quantum well (VQW) made by Si-donors crosses the Fermi level. Also, it is essential to reduce the distance between 2DEG and the surface of the heretostructure when fabricating HEMT, therefore  $d_{sp}$  should be minimized [16, 17].

Another approach to enhance the mobility is to increase Al content  $x$  in the  $\text{Al}_x\text{Ga}_{1-x}\text{As}$  barrier layer. But at  $x > 0.25$  electrons are strongly captured by DX-centers [18]. Moreover, the resistance of the ohmic contacts is also increasing with  $x$  increase.

In order not to increase  $d_{sp}$ , we proposed to introduce thin AlAs layers in a spacer layer AlGaAs. That will lead to displacement of the electron energy levels of the VQW above the Fermi level and prevent hybridization of the electron wave functions of QW and VQW. It should also be noted that AlAs is used as a stopper layer for wet etching and provides better selectivity instead of AlGaAs in HEMT. Nevertheless, the influence of AlAs on the scattering mechanisms of the Al-GaAs/InGaAs heterostructures with a composite spacer layer (CSP) AlGaAs/AlAs has not been studied yet.

The aim of the paper is to study the electron transport and scattering mechanisms in AlGaAs/InGaAs heterostructures with the CSP AlGaAs/AlAs. We proposed the CSP AlGaAs/AlAs with two AlAs inserts with thicknesses of 1 nm each. It is expected that the CSP will move the electron energy levels to the upper states in VQW made by Si-donors and allow enhancing the electron mobility in QW InGaAs.

## 2. Calculation of the band structure

The calculation of band structures was performed by the self-consistent solution of Schrödinger and Poisson equations in the effective mass approximation [19]. All calculations were conducted for temperature  $T = 300$  K. We used the following parameters: the effective electron masses of the conduction band  $0.041m_0$ ,  $0.081m_0$  and  $0.063m_0$  for  $\text{In}_{0.2}\text{Ga}_{0.8}\text{As}$ ,  $\text{Al}_{0.22}\text{Ga}_{0.78}\text{As}$  and GaAs, respectively, and the effective hole masses of the valence band  $0.41m_0$ ,  $0.57m_0$  and  $0.51m_0$  for  $\text{In}_{0.2}\text{Ga}_{0.8}\text{As}$ ,  $\text{Al}_{0.22}\text{Ga}_{0.78}\text{As}$  and GaAs, respectively [20, 21].

The conduction and valence band discontinuities at the heterointerface  $\text{Al}_{0.22}\text{Ga}_{0.78}\text{As}/\text{In}_{0.2}\text{Ga}_{0.8}\text{As}$  were equal to  $\Delta E_c = 0.5$  eV and  $\Delta E_v = 0.7$  eV, respectively, the value of a surface potential  $\varphi_s = 0.7$  eV. The Fermi energy  $E_F$  was at the zero level. The spacer layer  $\text{Al}_{0.22}\text{Ga}_{0.78}\text{As}$  thickness was  $d_{sp} = 6$  nm. The calculated band structure with the CSP AlGaAs/AlAs is presented in Fig. 1.

As seen in Fig. 1, the VQW does not cross  $E_F$  due to AlAs inserts. This means that the energy levels in the VQW are displaced to the upper states and preserve the appearance of the parallel conductivity in the AlGaAs barrier layer instead of the single spacer without AlAs inserts. Introduction of AlAs inserts also prevents the hybridization of the electron wave

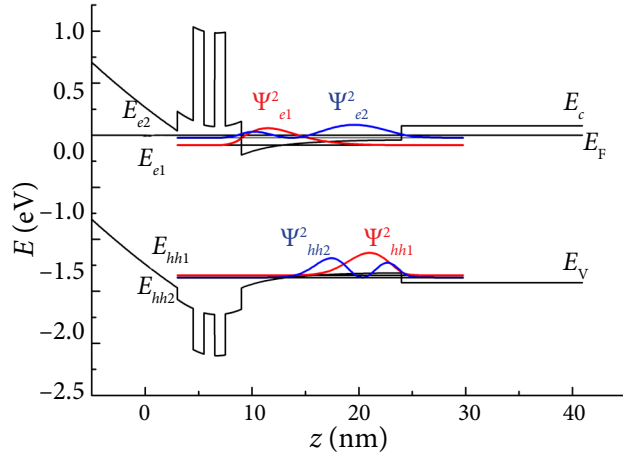


Fig. 1. Conduction and valence band structures and squared wave functions  $\psi_i$  of electrons and holes in QW InGaAs. Fermi energy  $E_F$  is at the zero level. A case of a composite spacer layer AlGaAs with two AlAs inserts.

functions of the QW and the VQW. We shall note that the CSP leads to a more effective electron confinement in the QW and also creates additional potential barriers that may reduce the leakage current.

### 3. Sample fabrication

The samples were grown by molecular-beam epitaxy on GaAs (100) wafers. The layout of the epi-layers is shown in Fig. 2.

Sample 416 contained a single spacer layer  $\text{Al}_{0.22}\text{Ga}_{0.78}\text{As}$  (see Fig. 2(a)) with a thickness  $d_{sp} = 5.5$  nm, while samples 417 and 440 were grown with a composite spacer layer  $\text{Al}_{0.22}\text{Ga}_{0.78}\text{As}$  with two AlAs inserts (see Fig. 2(b)) with  $d_{sp} = 5.5$  and 7.5 nm, respectively. The doping concentration

was  $N_D = 5.9 \times 10^{12} \text{ cm}^{-2}$  for samples 416, 417 and  $N_D = 5.4 \times 10^{12} \text{ cm}^{-2}$  for sample 440. The samples had one-side Si delta-doping, the QW  $\text{In}_{0.2}\text{Ga}_{0.8}\text{As}$  width was 11 nm and the AlAs inserts were 1 nm in size each. The buffer layer AlGaAs contained AlGaAs/GaAs superlattices (SLs) to preserve threading of defects from a substrate towards the growing layers.

The photoluminescence (PL) spectra were recorded using an optical cryostat in nitrogen atmosphere. The samples were mounted in a holder and kept at  $T = 77$  K. PL was excited by a continuous wave focused He-Ne laser radiation (632.8 nm) with excitation power up to 50 mW. The luminescence response in a spectral range  $1.2 < \hbar\omega < 1.6$  eV was detected by a cooled photomultiplier with S1-response [22]. The uncooled Hamamatsu InGaAs photodiode with a lock-in voltmeter was used.

### 4. Results and discussion

We measured the Shubnikov-de Haas (SdH) oscillations (magnetoresistance  $R_{xx}$ ) and the Hall resistance  $R_{xy}$  as a function of the applied magnetic field  $B$  at temperature of 4.2 K (see Fig. 3).

From the measured data we extracted the mobility  $\mu_e$  of 2DEG from which we calculated the transport scattering time using the relation  $\tau_t = \mu_e m^*/e$ . The electron effective mass for  $\text{In}_{0.2}\text{Ga}_{0.8}\text{As}$  was 0.041 times of the bare electron mass. The quantum scattering time  $\tau_q$  was determined from a Dingle style analysis [23]. It is well known that the amplitude of SdH oscillations  $\Delta R$  is described by the relation  $\Delta R \sinh(A_T)/4R_0 A_T = \exp(-\pi\omega_c \tau_q)$ , where  $A_T = 2\pi k_B T/\hbar\omega_c$  is the thermal damping factor, the cyclotron frequency is  $\omega_c = eB/m^*$ , and  $R_0$  is the zero-field resistance. Next we fitted a Dingle plot – the dependence

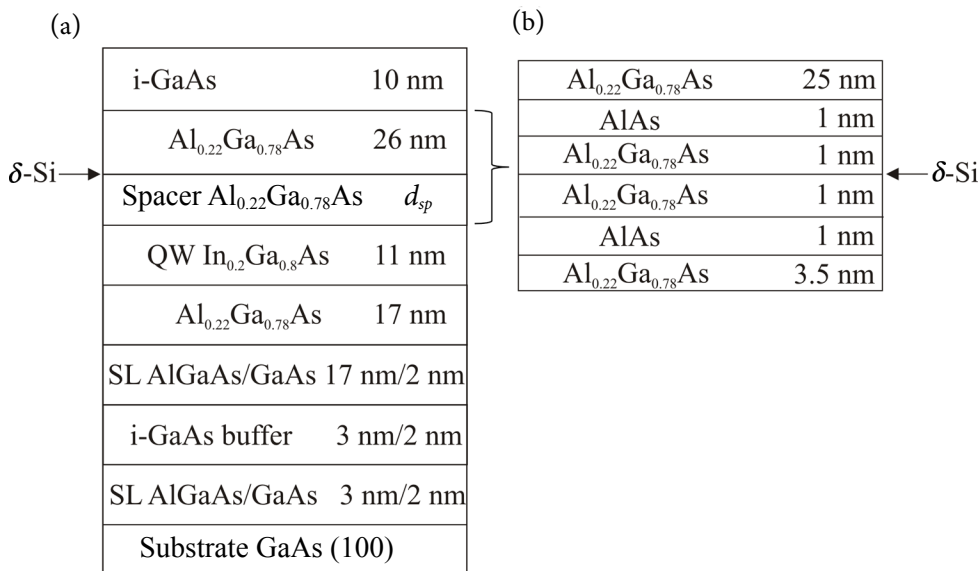


Fig. 2. The scheme of the grown heterostructures with the single spacer layer AlGaAs (a). The layout of the composite spacer layer AlGaAs with AlAs inserts is shown in (b).

of  $\Delta R \sinh(A_T)/4R_0 A_T$  in a log-scale versus  $1/B$  at a fixed temperature 4.2 K. The linear fit of a Dingle plot gives the slope  $s$  from which  $\tau_q$  can be extracted as  $\tau_q = \pi m^*/es$ . We have to notice that all the points in the Dingle plot should lie on a straight line. Usually there are 6–8 points and the relative error of  $\tau_q$  determination is about 5–6%. As shown in the inset in Fig. 3, all the points lie on an extrapolated straight line with a small deviation at high values of  $B$ . The results of determination of two scattering times and Hall measurements are indicated in Table 1.

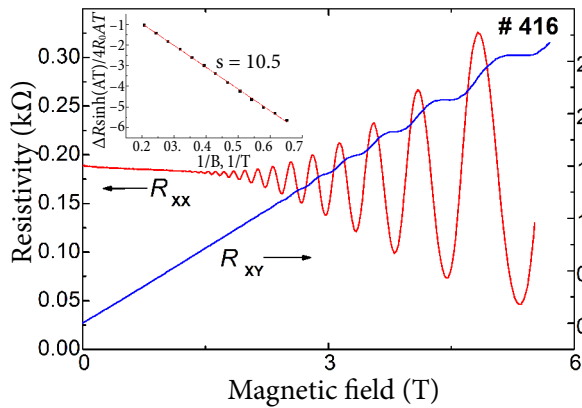


Fig. 3. The magnetoresistance  $R_{xx}$  and the Hall resistance  $R_{xy}$  as a function of the applied magnetic field  $B$  at temperature of 4.2 K. Inset corresponds to a Dingle plot from which the quantum scattering time  $\tau_q$  was extracted.

As seen, the  $\tau_l/\tau_q$  ratio increases significantly in sample 417 with a CSP AlGaAs/AlAs in comparison to sample 416 with the single spacer. That corresponds well with the Hall measurements for sample 417 that demonstrated mobility enhancement up to 20%. It should be noted that  $\tau_l/\tau_q \gg 1$  for all the samples. It means that the electron transport is substantially determined by the large-angle scattering and the dominant scattering factor is the scattering on ionized Si donors.

Sample 440 with the increased thickness of the CSP shows the highest mobility amongst all samples at  $T = 77$  K. We believe this is due to  $d_{sp}$  increase. In contrast,  $\tau_q$  has slightly increased in comparison with sample 417. The  $\tau_l/\tau_q$  ratio also demonstrates downturn behaviour. This can be explained by the following. On the one hand, with the  $d_{sp}$  increase the ionized Si-donors shall move further from the QW, but conversely this will move the VQW towards the Fermi level and the scattering will increase. Therefore the  $\tau_l/\tau_q$  ratio will slightly decrease but the electron mobility is enhanced.

It should be mentioned that introduction of AlAs inserts into the AlGaAs spacer layer did not affect the crystalline quality of the grown samples. Figure 4 demonstrates the PL spectra of sample 416 (with the single spacer) and sample 440 (with the CSP).

As seen, a strong thin peak on PL spectra with the energy  $\hbar\omega = 1.508$  eV corresponds to a nonradiative recombination in GaAs whereas a peak with  $\hbar\omega = 1.32$  eV is related to optical transitions in QW  $\text{In}_{0.2}\text{Ga}_{0.8}\text{As}$ . The energy region  $\hbar\omega = 1.65$ – $1.70$  eV relates to the optical transitions of the SL in the buffer layer AlGaAs.

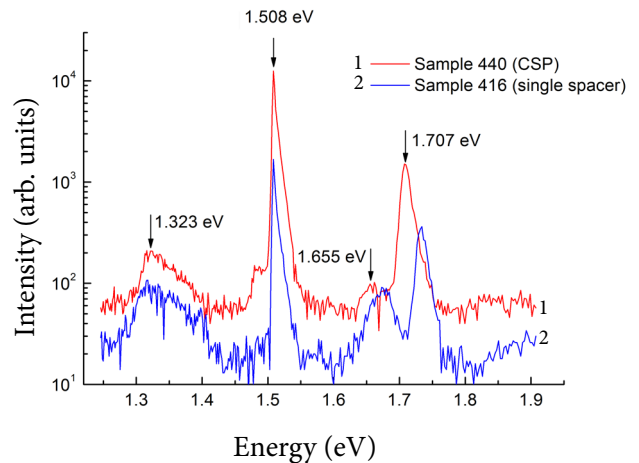


Fig. 4. PL spectra of samples 416 (lower, with the single spacer layer) and 440 (higher, with the CSP with  $d_{sp} = 7.5$  nm).

Table 1. Hall measurements and scattering time values for all the grown samples.

Sample	Spacer thickness $d_{sp}$ , nm	295 K		77 K		4.2 K
		$n_H \times 10^{12}$ , $\text{cm}^{-2}$	$\mu_H$ , $\text{cm}^2/\text{Vs}$	$n_H \times 10^{12}$ , $\text{cm}^{-2}$	$\mu_H$ , $\text{cm}^2/\text{Vs}$	$\tau_l/\tau_q$
416 (single spacer)	5.5	1.2	8780	1.7	34000	11.4
416 (CSP)	5.5	1.3	9500	1.8	36200	34.2
440 (CSP)	7.5	0.95	9070	1.28	38800	28.0

## 5. Conclusions

In this paper we have demonstrated that the introduction of nano-sized AlAs inserts to the composite spacer layer AlGaAs increases electron mobility up to 20% in comparison to the single spacer layer without AlAs inserts. The ratio of transport-to-quantum scattering times revealed this due to the decreased scattering on the ionized Si-donors and a strong confinement of electrons in the QW InGaAs.

## Acknowledgements

The work was partially supported by Contracts 02.G36.31.0005 and 33/211-13 in terms of Decree 218 of the Government of the Russian Federation.

## References

- [1] J. Požela, K. Požela, and V. Jucienė, Enhancement of electron drift velocity in a quantum well by confinement of polar optical phonons, *Phys. Status Solidi* **4**(2), 632–634 (2007), <http://dx.doi.org/10.1002/pssc.200673318>
- [2] K. Požela, Electron nonelastic scattering by confined and interface polar optical phonons in a modulation-doped AlGaAs/GaAs/AlGaAs quantum well, *Semicond.* **35**(11), 1305–1308 (2001), <http://dx.doi.org/10.1134/1.1418076>
- [3] J. Požela, K. Požela, V. Jucienė, A. Sužiedėlis, N. Žurauskienė, and A.S. Shkolnik, Electron transport in modulated-doped InAlAs/InGaAs/InAlAs and AlGaAs/InGaAs/AlGaAs heterostructures, *Lithuan. J. Phys.*, **51**(4), 270–275 (2011), <http://dx.doi.org/10.3952/physics.v51i4.2245>
- [4] V.A. Kulbachinskii, N.A. Yuzeeva, G.B. Galiev, E.A. Klimov, I.S. Vasilevskii, R.A. Khabibullin, and D.S. Ponomarev, Electron effective masses in an InGaAs quantum well with InAs and GaAs inserts, *Semicond. Sci. Tech.* **27**, 035021 (2012), <http://dx.doi.org/10.1088/0268-1242/27/3/035021>
- [5] J. Požela, K. Požela, and V. Jucienė, Electron mobility and electron scattering by polar optical phonons in heterostructure quantum wells, *Semicond.* **34**(9), 1011–1015 (2000), <http://dx.doi.org/10.1134/1.1309408>
- [6] J. Požela, K. Požela, and V. Jucienė, Scattering of electrons by confined interface polar optical phonons in a double-barrier heterostructure, *Semicond.* **41**(9), 1074–1079 (2007), <http://dx.doi.org/10.1134/S1063782607090126>
- [7] P. Lorenzini, Z. Bougrioua, A. Tiberj, R. Tauk, M. Azize, M. Sakowicz, K. Karpierz, and W. Knap, Quantum and transport lifetimes of two-dimensional electrons gas in AlGaAs/GaN heterostructures, *Appl. Phys. Lett.* **87**, 232107 (2005), <http://dx.doi.org/10.1063/1.2140880>
- [8] D. Schneider, L. Elbrecht, J. Creutzburg, A. Schlachetzki, and G. Zwinge, In-plane effective mass of electrons in InGaAs/InP quantum wells, *J. Appl. Phys.* **77**, 2828 (1995), <http://dx.doi.org/10.1063/1.358694>
- [9] L. Hsu and W. Walukiewicz, Transport-to-quantum lifetime ratios in AlGaAs/GaN heterostructures, *Appl. Phys. Lett.* **80**, 2508–2510 (2002), <http://dx.doi.org/10.1063/1.1468260>
- [10] T. Ando, A.B. Fowler, and F. Stern, Electronic properties of two-dimensional systems, *Rev. Mod. Phys.* **54**, 437 (1982), <http://dx.doi.org/10.1103/RevModPhys.54.437>
- [11] D. Sarma and F. Stern, Single-particle relaxation time versus scattering time in an impure electron gas, *Phys. Rev. B.* **32**, 8442(R), <http://dx.doi.org/10.1103/PhysRevB.32.8442>
- [12] M. McElhinney, B. Vögele, M.C. Holland, C.R. Stanley, E. Skuras, A.R. Long, and E.A. Johnson, 1.2 K Shubnikov–de Haas measurements and self-consistent calculation of silicon spreading in  $\delta$ - and slab-doped  $\text{In}_{0.53}\text{Ga}_{0.47}\text{As}$  grown by molecular beam epitaxy, *Appl. Phys. Lett.* **68**, 940 (1996), <http://dx.doi.org/10.1063/1.116105>
- [13] Y.M. Zhou, L.Y. Shang, G. Yu, K.H. Gao, W.Z. Zhou, T. Lin, S.L. Guo, J.H. Chu, N. Dai, and D.G. Austing, Transport properties of a spin-split two-dimensional electron gas in an  $\text{In}_{0.53}\text{Ga}_{0.47}\text{As}/\text{InP}$  quantum well structure, *Appl. Phys. Lett.* **106**, 073722 (2009), <http://dx.doi.org/10.1063/1.3244613>
- [14] M. Sakowicz, J. Lusakowski, K. Karpierz, M. Grynberg, and B. Majkusiak, Transport and quantum scattering time in field-effect transistors, *Appl. Phys. Lett.* **90**, 172104 (2007), <http://dx.doi.org/10.1063/1.2731713>
- [15] P.T. Coleridge, Small-angle scattering in two-dimensional electron gas, *Phys. Rev. B* **44**(8), 3793–3801 (1991), <http://dx.doi.org/10.1103/PhysRevB.44.3793>
- [16] R.A. Khabibullin, G.B. Galiev, E.A. Klimov, D.S. Ponomarev, I.S. Vasilevskii, V.A. Kulbachinskii, P.Yu. Bokov, L.P. Avakyants, A.V. Chervyakov, and P.P. Maltseva, Electrical and optical properties of near-surface AlGaAs/InGaAs/AlGaAs quantum wells with different quantum-well depths, *Semicond.* **47**(9), 1203–1208 (2013), <http://dx.doi.org/10.1134/S106378261309008X>
- [17] R.A. Khabibullin, I.S. Vasilevskii, D.S. Ponomarev, G.B. Galiev, E.A. Klimov, L.P. Avakyants, P.Yu. Bokov, and A.V. Chervyakov, the built-in electric field in PHEMT heterostructures with near-surface quantum wells  $\text{Al}_x\text{Ga}_{1-x}\text{As}/\text{In}_y\text{Ga}_{1-y}\text{As}/\text{GaAs}$ , *J. Phys. Conf. Ser.* **345**, 012015 (2012), <http://dx.doi.org/10.1088/1742-6596/345/1/012015>

- [18] S.B. Lisesivdin, H. Altuntas, A. Yildiz, M. Kasapa, E. Ozbay, and S. Ozelik, DX-center energy calculation with quantitative mobility spectrum analysis in n-AlGaAs/GaAs structures with low Al content, *Superlatt. Microstruct.* **45**(6), 604–611 (2009), <http://dx.doi.org/10.1016/j.spmi.2009.02.009>
- [19] D.S. Ponomarev, I.S. Vasilevskii, G.B. Galiev, E.A. Klimov, R.A. Khabibullin, V.A. Kulbachinskii, and N.A. Uzeeva, Electron mobility and effective mass in composite InGaAs quantum wells with InAs and GaAs nanoinserts, *Semicond.* **46**(4), 484–490 (2012), <http://dx.doi.org/10.1134/S1063782612040173>
- [20] W. Nakwaski, Effective masses of electrons and heavy holes in GaAs, InAs, AlAs and their ternary compounds, *Phys. B* **210**, 1–25 (1995), [http://dx.doi.org/10.1016/0921-4526\(94\)00921-H](http://dx.doi.org/10.1016/0921-4526(94)00921-H)
- [21] I. Vurgaftman, J.R. Meyer, and L.R. Ram-Mohan, Band parameters for III–V compound semiconductors and their alloys, *J. Appl. Phys.* **89**(11), 5815–5875 (2001), <http://dx.doi.org/10.1063/1.1368156>
- [22] R.A. Khabibullin, I.S. Vasilevskii, G.B. Galiev, E.A. Klimov, D.S. Ponomarev, V.P. Gladkov, V.A. Kulbachinskii, A.N. Klochkov, and N.A. Uzeeva, Effect of the built-in electric field on optical and electrical properties of AlGaAs/InGaAs/GaAs P-HEMT nanoheterostructures, *Semicond.* **45**(5), 657–662 (2011), <http://dx.doi.org/10.1134/S1063782611050162>
- [23] E. Diez, Y.P. Chen, S. Avesque, M. Hilke, E. Peled, D. Shahar, J.M. Cerver, D.L. Sivco, and A.Y. Cho, Two-dimensional electron gas in InGaAs/InAlAs quantum wells, *Appl. Phys. Lett.* **88**, 052107 (2006), <http://dx.doi.org/10.1063/1.2168666>

## KVANTINĖS IR ĮPRASTINĖS SKLAIDOS TRUKMĖS AlGaAs/InGaAs NANOHETERODARINIUOSE SU AlAs INTARPAIS BUFERINIAME SLUOKSNIJE

G.B. Galiev <sup>a</sup>, I.S. Vasilevskii <sup>b</sup>, E.A. Klimov <sup>a</sup>, D.S. Ponomarev <sup>a</sup>, R.A. Khabibullin <sup>a</sup>,  
V.A. Kulbachinskii <sup>c</sup>, D.V. Gromov <sup>b</sup>, P.P. Maltsev <sup>a</sup>

<sup>a</sup> *Rusijos mokslų akademijos Superaukšto dažnio puslaidininkų elektronikos institutas, Maskva, Rusija*

<sup>b</sup> *Nacionalinio branduolinių mokslinių tyrimų universiteto Maskvos inžinerinės fizikos institutas, Maskva, Rusija*

<sup>c</sup> *Valstybinis Maskvos M. V. Lomonosovo universitetas, Maskva, Rusija*